

Dispelling Rayleigh's Curse

J. Rehacek,¹ M. Paúr,¹ B. Stoklasa,¹ L. Motka,¹ Z. Hradil,¹ and L. L. Sánchez-Soto^{2,3}

¹Department of Optics, Palacký University, 17. listopadu 12, 771 46 Olomouc, Czech Republic

²Departamento de Óptica, Facultad de Física, Universidad Complutense, 28040 Madrid, Spain

³Max-Planck-Institut für die Physik des Lichts, Günther-Scharowsky-Straße 1, Bau 24, 91058 Erlangen, Germany

We devise a systematic method to determine the Fisher information required for resolving two incoherent point sources with a diffraction-limited linear imaging device. The resulting Cramér-Rao bound gives the lowest variance achievable for an unbiased estimator. When only intensity in the image plane is recorded, this bound diverges as the separation between the sources tends to zero, an effect which has been dubbed as Rayleigh's curse. However, this curse can be lifted using suitable coherent measurements. In particular, we determine a class of measurements that can be easily implemented as projections on the orthogonalized derivatives of the point spread function of the system.

PACS numbers: 03.65.Ta, 03.67.-a, 42.50.St

Introduction.— The spatial resolution of any imaging device is restricted by light diffraction [1], which causes a sharp point on the object to blur into a finite-sized spot in the image. This information is encoded in the point spread function (PSF) [2], whose size determines the resolution: two points closer than the PSF width will be difficult to resolve due to the substantial overlap of their images. This is the physical significance of the famous Rayleigh criterion [3].

Needless to say, improving this limit is a source of continuing research. Actually, in the past two decades a number of top-notch techniques have appeared, overcoming Rayleigh's limit under particular conditions. They rely on nonconventional strategies, such as near-field imaging or on nonclassical or nonlinear optical properties of the object [4–10]. However, these schemes are often challenging and require careful control of the source, which is not always possible.

Quite recently, Tsang and coworkers [11–13] have re-examined this question from the perspective of estimation theory. The idea is to use the Fisher information and the associated Cramér-Rao lower bound (CRLB) to quantify how well the separation between two poorly resolved incoherent point sources can be estimated. When only light intensity at the image plane is measured (the basis of all the traditional techniques), the Fisher information falls to zero as the separation between the sources decreases and the CRLB diverges accordingly; this is Rayleigh's curse [11]. On the other hand, when the Fisher information of the complete field is calculated, it remains constant and so does the CRLB, which implies that the Rayleigh limit is subsidiary to the problem.

These stunning predictions prompted a sequence of rapid-fire experimental implementations [14–17]. Nonetheless, these proposals have some limitations, for the detection works only for small separations or is limited to particular source profiles. Inspired by these developments, we establish in this Letter a general procedure to construct optimal measurements (see also the recent related work [18]). By this, we mean spatial modes such that, when the signal is projected onto them, they yield a constant Fisher information thus attaining the CRLB; i.e., the separation can be estimated with the best achievable precision.

The key feature of these modes is the spatial symmetry. Even more interestingly, we determine detection schemes achieving the quantum limit for any symmetric PSF: the associated modes turn out to be orthogonal polynomials with respect to a measure that is just the PSF.

Model and measurements.— We follow the basic model of Tsang and coworkers [11–13] and consider quasimonochromatic paraxial waves with one specified polarization and one spatial dimension, x , denoting the image-plane coordinate. We formulate what follows in a quantum language, even though it can be directly applied to a classical scenario. A coherent complex amplitude $U(x)$ can be assigned to a ket $|U\rangle$, such that $U(x) = \langle x|U\rangle$, where $|x\rangle$ represents a point-like source located at x .

We take a spatially-invariant imaging system. The associated PSF, which is just the normalized intensity response to a point light source, is denoted as $I(x) = |\langle x|\Psi\rangle|^2 = |\Psi(x)|^2$, where $\Psi(x)$ is the amplitude PSF, which we require to be inversion symmetric; i.e., $\Psi(x) = \Psi(-x)$, an assumption met by most aberration-free imaging systems.

Two incoherent point sources, each of the same intensity, are located at two unknown points $X_{\pm} = \pm s/2$ in the object plane. This regular configuration entails no essential loss of generality. Our objective is to estimate the separation $s = X_+ - X_-$.

The density matrix for the image-plane modes is thus

$$\rho_s = \frac{1}{2}(|\Psi_+\rangle\langle\Psi_+| + |\Psi_-\rangle\langle\Psi_-|), \quad (1)$$

where the spatially-shifted responses are $\Psi_{\pm}(x) = \langle x \pm s/2|\Psi\rangle$. This density matrix gives the normalized mean intensity profile: $\rho_s(x) = \frac{1}{2}(|\Psi(x-s/2)|^2 + |\Psi(x+s/2)|^2)$. The spatial modes excited by the two sources are not orthogonal, in general ($\langle\Psi_-|\Psi_+\rangle \neq 0$), which means that they cannot be separated by independent measurements. This is the crux of the problem.

To estimate s we must perform appropriate measurements. Complete von Neumann tests [19] will prove sufficient for our purposes. They consist of a set of orthonormal projectors $\{|n\rangle\langle n|\}$ (with $\langle n|n'\rangle = \delta_{nn'}$) resolving the identity

$\sum_n |n\rangle\langle n| = \mathbb{1}$. Each projector represents a single output channel of the measuring apparatus; the probability of detecting the n th output is given by the Born rule $p_n(\mathfrak{s}) = \langle n|\rho_{\mathfrak{s}}|n\rangle$. The generalization to continuous observables is otherwise straightforward.

The statistics of the quantum measurement carries information about \mathfrak{s} . This is aptly encompassed by the Fisher information [20, 21], which is a mathematical measure of the sensitivity of an observable quantity to changes in its underlying parameters (the emitter's position). It is defined as

$$\mathcal{F}_{\mathfrak{s}} = \mathbb{E} \left[\left(\frac{\partial \log p_n(\mathfrak{s})}{\partial \mathfrak{s}} \right)^2 \right], \quad (2)$$

with $\mathbb{E}[Y]$ being the expectation value of the random variable Y . The Cramér-Rao lower bound (CRLB) [22, 23] ensures that the variance of any unbiased estimator $\hat{\mathfrak{s}}$ of the quantity \mathfrak{s} is bounded by the reciprocal of the Fisher information; viz,

$$\text{Var}(\hat{\mathfrak{s}}) \geq \frac{1}{\mathcal{F}_{\mathfrak{s}}}. \quad (3)$$

Let us take the von Neumann measurement as the continuous projection over $|x\rangle\langle x|$, which corresponds to conventional image-plane intensity detection (or photon counting, in the quantum regime). We stress that this is the information used in any traditional technique, including previous superresolution approaches. The Fisher information (per detection event) for this scheme reads as

$$\mathcal{F}_{\mathfrak{s}} = \int_{-\infty}^{\infty} \frac{1}{\rho_{\mathfrak{s}}(x)} \frac{\partial^2 \rho_{\mathfrak{s}}(x)}{\partial \mathfrak{s}^2} dx \simeq \mathfrak{s}^2 \int_{-\infty}^{\infty} \frac{[I''(x)]^2}{I(x)} dx, \quad (4)$$

where, in the second integral we have performed a first-order expansion in \mathfrak{s} , which is valid only for points sufficiently close together. Then, $\mathcal{F}_{\mathfrak{s}}$ goes to zero quadratically as $\mathfrak{s} \rightarrow 0$. This means that detection of intensity at the image plane is progressively worse at estimating the separation for closer sources, to the point that the variance in this situation is doomed to blow up.

To bypass this obstruction, we need a different measurement that incorporates the information available in the phase discarded by the intensity detection. In what follows we require our measurement to have a well-defined parity; i.e., $\langle -x|n\rangle = \pm \langle x|n\rangle$. Accordingly,

$$p_n \equiv |a_n|^2 = |\langle n|\Psi_{\pm}\rangle|^2, \quad (5)$$

so that the measurement does not feel the two-component structure of the signal. Additionally, the probability amplitudes a_n have to fulfill

$$\text{Im} \left(a_n \frac{\partial a_n^*}{\partial \mathfrak{s}} \right) = 0. \quad (6)$$

This property allows one to write the Fisher information as

$$\mathcal{F}_{\mathfrak{s}} = 4 \sum_n \left| \frac{\partial a_n}{\partial \mathfrak{s}} \right|^2. \quad (7)$$

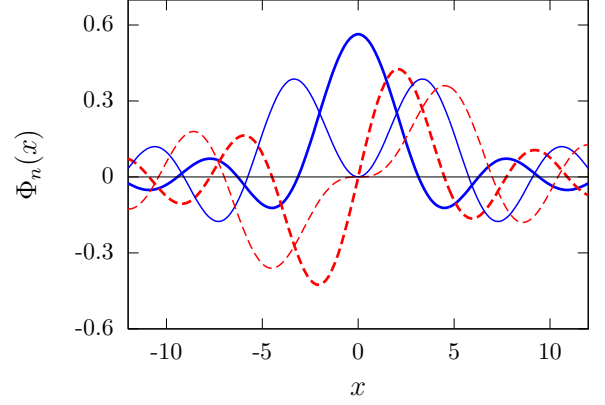


FIG. 1. First PSF-adapted modes (14) for a sinc response. In blue solid lines we plot the symmetric modes [$n = 0$ (thick) and $n = 2$ (thin)] and in red broken lines we have the antisymmetric ones [$n = 1$ (thick) and $n = 3$ (thin)].

Next, we note that $|\Psi_{\pm}\rangle = \exp(\pm i s P/2)|\Psi\rangle$. Here, P is the momentum operator that generates displacements in the x variable, so it acts as a derivative $P = -i\partial_x$, much in the same way as in quantum optics. Because of the completeness of the eigenstates of P , Eq. (5) can be rewritten in the form

$$a_n = \int \langle n|p\rangle \langle p|\Psi\rangle e^{-i s p/2} dp. \quad (8)$$

Inserting this in (7), performing the derivative, and using measurement completeness, we finally obtain the compact expression

$$\mathcal{F}_{\mathfrak{s}} = \int p^2 |\Psi(p)|^2 dp = \langle P^2 \rangle, \quad (9)$$

where $\Psi(p)$ is the Fourier transform of the PSF amplitude $\Psi(x)$. The Fisher information appears then as the second moment of the momentum with respect to the PSF and is therefore independent of the separation of the points. Consequently, the variance in the CRLB remains constant and one lifts Rayleigh's curse, as heralded. Incidentally, Eq. (9) is known to be the ultimate quantum limit [24, 25]. Hence, we have clearly identified conditions enabling a measurement to attain the quantum CRLB. This is the first main result of this Letter.

Before proceeding further, we return to Eq. (6). This condition is readily satisfied by choosing $a_n = |a_n| \exp(i\alpha_n)$, with phases α_n independent of \mathfrak{s} . As these phases can be absorbed in the basis $|n\rangle$, this is tantamount to requiring real probability amplitudes a_n . Due to the properties of the Fourier transform, this imposes

$$\langle n|p\rangle \langle p|\Psi\rangle = \pm (\langle n|p\rangle \langle p|\Psi\rangle)^*, \quad (10)$$

where the symmetries of the PSF amplitude and the measurement have been employed. Hence a sufficient condition to enabling (6) is that the diagonal elements of the operators $|\Psi\rangle\langle n|$

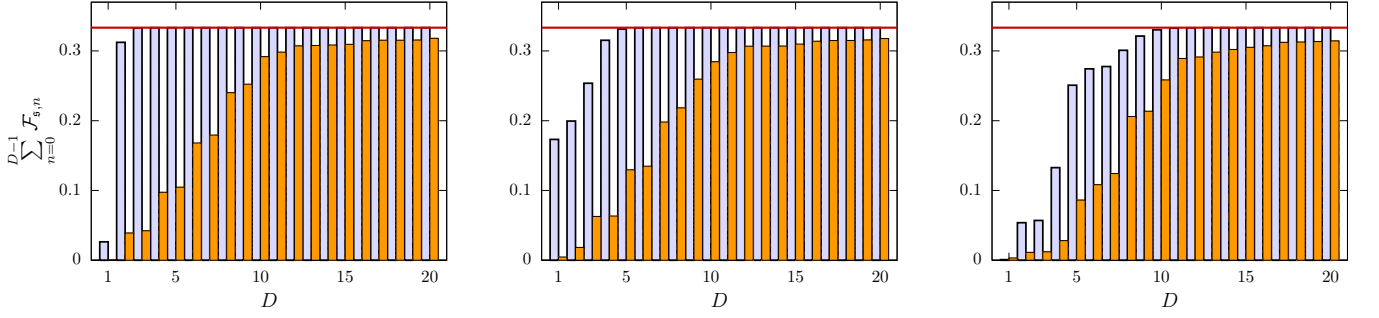


FIG. 2. Fisher information attained by the first D projections on the Hermite-Gauss basis with arbitrarily chosen $\sigma = \pi$ (orange bars) and the PSF-adapted measurement (14), when applied to a system with a sinc impulse response. The plots are for separations $\varsigma = 1$ (left), $\varsigma = 2$ (middle), and $\varsigma = 15$ (right), and the corresponding Rayleigh limit is $\varsigma = \pi$. More than a hundred of Hermite-Gauss projections must be measured to access 98.5% of the quantum Fisher information (indicated by a horizontal red line) for $\varsigma = [0, 15]$, whereas just ten projections of the PSF-adapted measurement are sufficient.

in the momentum representation are all real or purely imaginary. For a real PSF amplitude, an obvious choice of $|n\rangle$ is a complete set of real wave functions $\langle x|n\rangle$ with a well-defined parity (symmetric or antisymmetric). The position projection (i.e., intensity detection) does not have the required symmetry and this explains why the intensity scan fails to reach the quantum bound.

Optimal strategies.— It is known that the optimal measurement in the limit of small ς is proportional to the first derivative of $\Psi(x)$ [17]. This suggests that one could try to project the signal on a set of orthonormalized derivatives of $\Psi(x)$. Indeed, we propose to construct the measurement basis $|n\rangle$ in momentum space as

$$\Phi_n(p) \equiv \langle p|n\rangle = Q_n(p)\Psi(p), \quad (11)$$

where $Q_n(p)$ is a system of orthogonal polynomials, with respect to the measure $|\Psi(p)|^2 dp$. Since this measure is symmetric, they satisfy the symmetry property $Q_n(-p) = (-1)^n Q_n(p)$ [26].

One can check that this generates a *bona fide* measurement basis. Truly, for the states (11), the condition (10) trivially holds, the probability amplitudes $a_n = \langle n|\Psi_{\pm}\rangle$ are real, and (6) is fulfilled. Of course, one would expect that the number of significant projections is small, and even the first derivative is sufficient in the superresolution regime.

The optimal PSF-adapted modes attaining the CRLB (9) for all separations are obtained by an inverse Fourier transform

$$\Phi_n(x) \equiv \langle x|n\rangle = \frac{1}{\sqrt{2\pi}} \int Q_n(p)\Psi(p)e^{ipx} dp. \quad (12)$$

The general rules (11) and (12) of finding the PSF-optimized scheme make the second main result of this Letter.

As a first, important example, we consider a Gaussian PSF amplitude $\Psi(x) = (2\pi)^{-1/4} \exp(-x^2/4)$, with unit variance ($\sigma = 1$). The Fourier transform is again a Gaussian, and a direct calculation gives $\mathcal{F}_{\varsigma} = 1/4$. The optimal PSF-adapted set consists of Hermite-Gauss polynomials, which are orthonormal with respect to the PSF.

As a second example, we take a slit aperture with $\Psi(x) = \frac{1}{\sqrt{\pi}} \text{sinc}(x)$ and Fourier transform $\Psi(p) = \frac{1}{\sqrt{2}} \text{rect}(p/2)$. Here, $\text{sinc}(x) = \sin(x)/x$ and $\text{rect}(p)$ is 0 outside the interval $[-1/2, 1/2]$ and 1 inside it. The set $\Phi_n(p)$ is now the Legendre polynomials $L_n(p)$, which are complete in the unit interval. In this way,

$$a_n = \langle n|\Psi_{\pm}\rangle = \frac{\sqrt{2n+1}}{2} \int_{-1}^1 L_n(p) e^{-ips/2} dp. \quad (13)$$

By Eq. (9), the Fisher information is $\mathcal{F}_{\varsigma} = 1/3$ and, by (12), the optimal measurement modes are given as

$$\Phi_n(x) = \sqrt{n+1/2} \frac{J_{n+1/2}(x)}{\sqrt{x}}, \quad (14)$$

where $J_k(x)$ is the Bessel function of the first kind. For $n = 1$, the measurement reduces to the first derivative of the sinc function, as expected. In Fig. 1 we plot the first PSF-adapted modes (14).

Each projection contributes with a piece of information

$$\mathcal{F}_{\varsigma,n} = \frac{\pi \left[nJ_{n-\frac{1}{2}}(\varsigma/2) - (n+1)J_{n+\frac{3}{2}}(\varsigma/2) \right]^2}{(2n+1)\varsigma}, \quad (15)$$

and, interestingly enough, all these complicated terms sum up to a total of $\mathcal{F}_{\varsigma} = 1/3$.

If the PSF amplitude of the system is real, any complete set of real modes with defined parity will also work. For example, the sinc response will also be optimal with a projection on Hermite-Gauss modes, but the connection to derivatives is lost. Besides, it might happen that, for small separations, the number of significant projections will be much larger than for the PSF-adapted set.

This can be illustrated by comparing the performances of different sets of measurements for the same PSF. Assuming a sinc, we can compare two optimal sets: the PSF-adapted measurement of Eq. (14) and the Hermite-Gauss projections. Figure 2 shows the information obtained by summing the Fisher

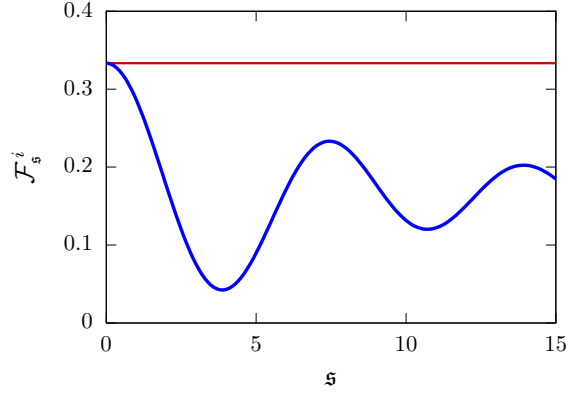


FIG. 3. Fisher information accessed by measuring the Fourier sine transform of two incoherent images separated by a distance s for a sinc impulse response. Notice that for small separations this measurement is optimal. For larger separations the complement of \mathcal{F}_s^i to quantum Fisher information is accessed by the Fourier cosine transform.

information over the first D projections. Both measurements attain the quantum CRLB; however, the number of effective projections to be measured is considerably less for the optimized measurement. We can also see that this advantage decreases with increasing separations.

Another feasible option is to project in modes comprised of the real and imaginary parts of plane waves; i.e.,

$$\Phi_k^r(x) = \frac{1}{\sqrt{2\pi}} \cos(kx), \quad \Phi_k^i(x) = \frac{1}{\sqrt{2\pi}} \sin(kx), \quad (16)$$

where now the modes are indexed by the continuous wave vector k . This can be implemented using the Fourier properties of optical lenses and spatial light modulators. In Fig. 3 we plot the Fisher information corresponding to

$$\mathcal{F}_s^i = \frac{1}{2} \int_{-1}^1 k^2 \sin^2\left(\frac{ks}{2}\right) dk, \quad (17)$$

obtained by such a measurement for different separations. For small separations, the imaginary part of the signal spectrum alone readily provides all the available information. Again, we note that in this limit the same information can be extracted with a single projection of the PSF-optimized measurement (14).

Concluding remarks.— In conclusion, we have shown that optimal sub-Rayleigh two-point resolution can be achieved with an optical system having a symmetric amplitude PSF provided the system output is projected onto a suitable complete set of modes with definite parity. Particularly useful modes can be generated from the derivatives of the system PSF, which in the limit of small separation can access all available information with a single projection.

The above formalism can be generalized to other transformations provided the frequency spectrum is replaced with a

suitable representation, in which the assumed transformation becomes a simple phase shift.

Acknowledgments.— We thank Gerd Leuchs, Olivia Di Matteo, and Matthew Foreman for valuable discussions and comments. Encouraging exchanges with Mankei Tsang are also appreciated. We acknowledge financial support from the Technology Agency of the Czech Republic (Grant TE01020229), the Grant Agency of the Czech Republic (Grant No. 15-03194S), the IGA Project of the Palacký University (Grant No. IGA PrF 2016-005) and the Spanish MINECO (Grant FIS2015-67963-P).

-
- [1] E. Abbe, “Ueber einen neuen Beleuchtungsapparat am Mikroskop,” *Arch. Mikrosk. Anat.* **9**, 469–480 (1873).
 - [2] J. W. Goodman, *Introduction to Fourier Optics* (Roberts and Company, Englewood, 2004).
 - [3] Lord Rayleigh, “Investigations in optics, with special reference to the spectroscope,” *Phil. Mag.* **8**, 261–274 (1879).
 - [4] A. J. den Dekker and A. van den Bos, “Resolution: a survey,” *J. Opt. Soc. Am. A* **14**, 547–557 (1997).
 - [5] S. W. Hell, “Far-field optical nanoscopy,” *Science* **316**, 1153–1158 (2007).
 - [6] M. I. Kolobov, “Quantum Imaging,” (Springer, Berlin, 2007) Chap. Quantum Limits of Optical Super-Resolution, pp. 113–138.
 - [7] Focus issue: Super-resolution Imaging, *Nat. Photonics* **3**, 361–420 (2009).
 - [8] S. W. Hell, “Microscopy and its focal switch,” *Nat. Meth.* **6**, 24–32 (2009).
 - [9] G. Patterson, M. Davidson, S. Manley, and J. Lippincott-Schwartz, “Superresolution imaging using single-molecule localization,” *Annu. Rev. Phys. Chem.* **61**, 345–367 (2010).
 - [10] C. Cremer and R. B. Masters, “Resolution enhancement techniques in microscopy,” *Eur. Phys. J. H* **38**, 281–344 (2013).
 - [11] M. Tsang, R. Nair, and X.-M. Lu, “Quantum theory of superresolution for two incoherent optical point sources,” [arXiv:1511.00552](#) (2015).
 - [12] R. Nair and M. Tsang, “Ultimate quantum limit on resolution of two thermal point sources,” [arXiv:16004.00937](#).
 - [13] S. Z. Ang, R. Nair, and M. Tsang, “Quantum limit for two-dimensional resolution of two incoherent optical point sources,” [arXiv:1606.00603](#).
 - [14] T. Z. Sheng, K. Durak, and A. Ling, “Fault-tolerant and finite-error localization for point emitters within the diffraction limit,” [arXiv:1605.07297](#).
 - [15] F. Yang, A. Taschilina, E. S. Moiseev, C. Simon, and A. I. Lvovsky, “Far-field linear optical superresolution via heterodyne detection in a higher-order local oscillator mode,” [arXiv:1606.02662](#).
 - [16] W. K. Tham, H. Ferretti, and A. M. Steinberg, “Beating Rayleigh’s curse by imaging using phase information,” [arXiv:1606.02666](#).
 - [17] M. Paur, B. Stoklasa, Z. Hradil, L. L. Sanchez-Soto, and J. Rehacek, “Achieving quantum-limited optical resolution,” [arXiv:1606.08332](#).
 - [18] C. Lupo and S. Pirandola, “Ultimate precision limits for quantum sub-Rayleigh imaging,” [arXiv:1604.07367](#).
 - [19] A. Peres, *Quantum Theory: Concepts and Methods* (Kluwer, New York, 2002).

- [20] R. A. Fisher, “Theory of statistical estimation,” [Math. Proc. Cambridge](#) **22**, 700–725 (1925).
- [21] D. Petz and C. Ghinea, “Introduction to Quantum Fisher Information,” in [Quantum Probability and Related Topics](#), Vol. Volume 27 (World Scientific, 2011) pp. 261–281.
- [22] C. W. Helstrom, *Quantum Detection and Estimation Theory* (Academic, New York, 1976).
- [23] A. S. Holevo, *Probabilistic and Statistical Aspects of Quantum Theory*, 2nd ed. (North Holland, Amsterdam, 2003).
- [24] S. L. Braunstein and C. M. Caves, “Statistical distance and the geometry of quantum states,” [Physical Review Letters](#) **72**, 3439–3443 (1994).
- [25] M. G. A. Paris, “Quantum estimation for quantum technology,” [Int. J. Quantum Inform.](#) **07**, 125–137 (2009).
- [26] G. Szegő, *Orthogonal Polynomials*, Colloquium Publications, Vol. XXIII (American Mathematical Society, Providence, 1938).